A Bayesian Marked Hierarchical Spatial Point Process Model with Covariates for Lesion Data

Bernd Taschler[1], Jian Kang[2], Kerstin Bendfeldt[3], Jens Wuerfel[3], Timothy D Johnson[2], and Thomas E Nichols[4]

[1]Centre for Complexity Science, University of Warwick, Coventry, UK, [2]Department of Biostatistics, University of Michigan, Ann Arbor, Michigan, USA, [3]Medical Image Analysis Center, Basel, Switzerland, [4]Department of Statistics, University of Warwick, Coventry, UK.

Background

Multiple Sclerosis (MS) is a chronic inflammatory-demyelinating disease of the central nervous system. MS patients can be grouped into four distinct clinical categories (CIS, RRMS, SPMS, PPMS), according to disease pathology. Currently, evaluation of MS with MRI data is largely qualitative, assessing existence and general location of lesions. We present a quantitative classification method of MS subtype using a hierarchical, fully Bayesian spatial point process model for lesion location, including covariates and lesion-specific attributes.

Methods (I): Hierarchical Poisson/Gamma Random Field Model

- A statistical approach where both the location and the number of data points is random.
- A doubly stochastic Poisson point process is driven by an intensity function (Fig.1).

Model. Denote a **Poisson point process** $\mathbf{Y}_j$ with intensity measure $\Lambda_j(dy)$ on $\mathcal{B} \subseteq \mathbb{R}^3$ for each MS subtype j as

$$[\mathbf{Y}_j|\Lambda_j(dy)] = \mathcal{PP}\{\mathcal{B}, \Lambda_j(dy)\}, \tag{1}$$

where the intensity measure for subtype j

$$\Lambda_j(dy) = \int_{\mathcal{B}} K_{\sigma_j^2}(dy, x) G_j(dx) \tag{2}$$

is a convolution of a Gamma random field and a **Gaussian kernel** $K_{\sigma_j^2}(dy, x)$.

The subtype **gamma random fields** $G_j(dx)$ are hierarchically defined as

$$[G_j(dx)|G_0(dx), \tau] \overset{iid}{\sim} \mathcal{GRF}\{G_0(dx), \tau\}, \tag{3}$$

$$[G_0(dx)|\alpha(dx), \beta] \sim \mathcal{GRF}\{\alpha(dx), \beta\}, \tag{4}$$

where $G_0(dx)$ represents a common, population-level gamma random field.

$$[(\mathbf{X}_j, \mathbf{Y}_j)|\{(\eta_{j,m}, \theta_m)\}, \sigma_j^2] \sim \mathcal{PP}\left\{\mathcal{B}, K_{\sigma_j^2}(dy, x) \sum_{m=1}^{M} \eta_{j,m} \delta_{\theta_m}(dx)\right\} \tag{5}$$

$$[\eta_{j,m}|\nu_m, \tau] \overset{iid}{\sim} \Gamma(\nu_m, \tau); \qquad \{(\theta_m, \nu_m)\}_{m=1}^{M} \sim \text{invLévy}\{\alpha(dx), \beta\} \tag{6}$$

Methods (II): The Intensity-Marked Model

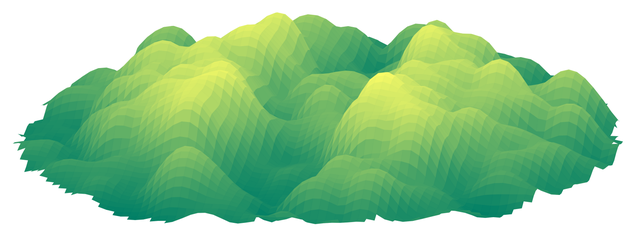

Fig. 1: 2D projection of the intensity that is driving the point process. It is modelled via a convolution of a Gamma random field with a Gaussian kernel.

Covariates. Point process intensities can be related to subject-specific attributes by introducing spatially constant covariates such as demographic data or clinical scores. Contributions from covariates to the intensity function are multiplicative with a log-link dependence as in univariate Poisson regression models.

Marks. Additional information about individual lesions can be incorporated by attaching a *mark* to every point location. In the simplest case, the distribution of marks is estimated independently from their respective point locations. In order to allow marks to inform the spatial intensity we model the marks using a log-Normal distribution with parameters depending on the intensity function (see Fig. 2).

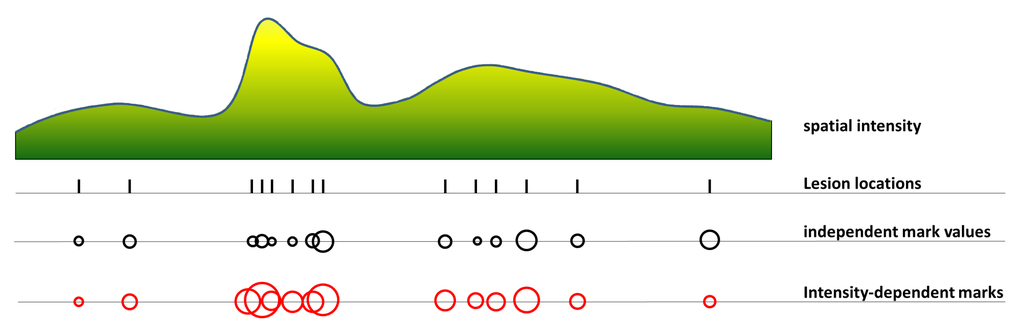

Fig. 2: Illustration of intensity-dependent marks in 1D. Mark values are inflated or shrunk according to the estimated spatial intensity at their location.

Bayesian Inference. We use **MCMC** techniques to sample from the full posterior distribution and estimate the intensity maps; and an importance sampling approach [2] to perform leave-one-out cross-validation.

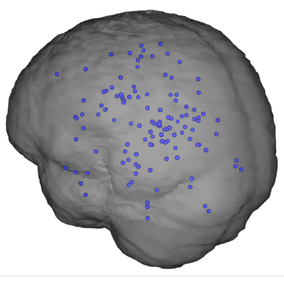

Fig. 3: Lesion locations forming a spatial point pattern.

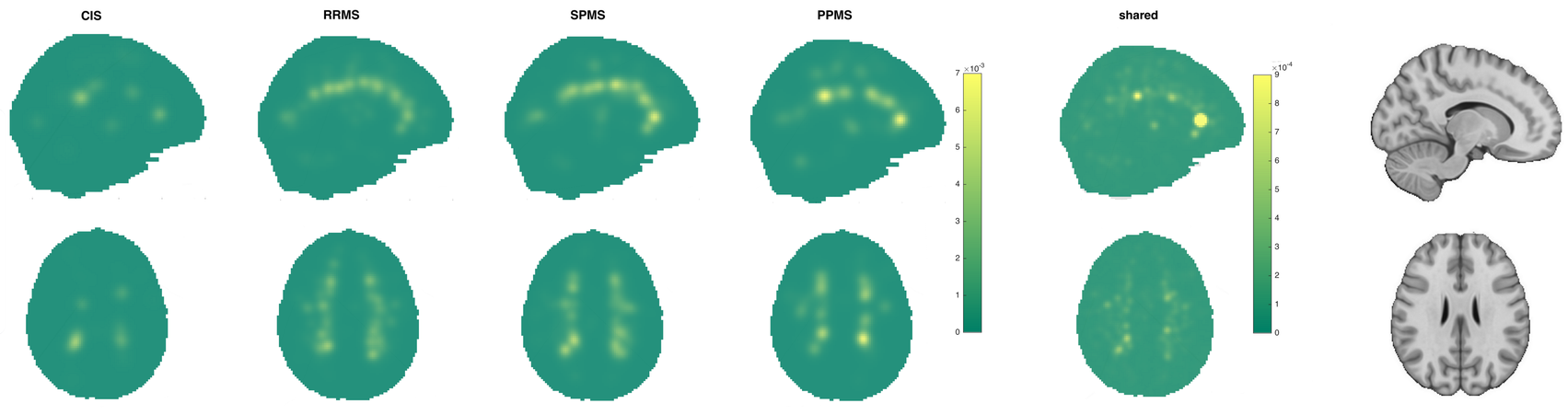

Fig. 4: Estimated mean posterior intensity maps; based on lesion locations derived from T2-weighted MR images.

Application: Multiple Sclerosis Lesion Data

Data. 238 subjects were scanned on a 1.5T Siemens Avanto scanner, collecting T_2-weighted images; native resolution was $0.9766 \times 0.9766 \times 3.0\text{mm}^3$. Lesion masks were created in native space by a semi-automatic procedure [3] and affine registered to MNI space. Lesion centres of mass were extracted using FSL; total number of lesions: 8064. Clinical categorisation (MS subgroups) was CIS:10, RRMS:172, SPMS:43, PPMS:13.
Covariates. Demographic (age, sex) and clinical measures (disease duration, EDSS, PASAT scores).
Marks. Individual lesion volume. Other potential candidates: Surface area, width, texture features, etc.
Results. 2D-slices of estimated mean posterior intensity maps are shown in Fig. 4. The computed intensities are consistent with empirically obtained binary lesion maps. Model validation via LOOCV shows high classification accuracies of 90.8% (classification into one of four MS subtypes, balanced for group sizes). Importantly, our spatially informed model performs better than a machine learning approach using support vector machine (56%) as well as a full-image probit regression model (82%) [5]. The addition of individual lesion volume as marks marginally increases prediction accuracy.

Discussion & Outlook

- Our approach uses a non-parametric Bayesian spatial point process model for inference and classification/prediction.
- Due to its non-parametric nature, the model provides greater flexibility in estimating the underlying intensity function (in essence a probability map) than parametric approaches.
- Despite using only lesion location, it has accuracy similar to using all image data, while being less dependent on exact lesion segmentation.
- Future work: multivariate mark distributions, spatially varying covariates (e.g. a white-matter mask).

contact: b.taschler@warwick.ac.uk
@bathybicBee

our group: http://warwick.ac.uk/tenichols/ohbm

References
[1] Ho, Stoyan (2008), *Stat Probabil Lett* 78: 1994-1999.
[2] Kang J, et al. (2014), *Ann of Appl Stat* 8 (3): 1800-1824.
[3] Kappos L, et al. (2006), *NEJM* 335 (11): 1124-1140.
[4] Møller J, et al. (1998), *Scand J Stat* 25: 451-482.
[5] Taschler B, et al. (2014), *LNCS - MICCAI 2014* 8674: 797-804.
[6] Wolpert RL, et al. (1998), *Biometrika* 85 (2): 251-267.